Chemical Engineering Science 66 (2011) 2912–2919

Contents lists available at ScienceDirect

Chemical Engineering Science

journal homepage: www.elsevier.com/locate/ces

Ideal micromixing performance in packed microchannels

Yuanhai Su, Guangwen Chen *, Quan Yuan

Dalian National Laboratory for Clean Energy, Dalian Institute of Chemical Physics, Chinese Academy of Sciences, Dalian 116023, China

ARTICLE INFO

Article history:
Received 23 October 2010
Received in revised form
8 January 2011
Accepted 14 March 2011
Available online 21 March 2011

Keywords:
Mixing
Microchannel
Process intensification
Fluid mechanics
Packed bed
Diffusion

ABSTRACT

In this work, the hydrodynamics and the micromixing characteristics in the packed and non-packed microchannels were studied experimentally at low Reynolds numbers (8–300). The mixing performances in microchannels were observed with high-speed CCD camera, and were evaluated in terms of a segregation index by the Villermaux/Dushman method. The fluid elements were drastically stretched, folded, and sheared with the effects of micro-particles in packed microchannels, resulting in extremely shorter diffusion distance and larger effective interfacial area, and much higher micromixing efficiency compared with those of non-packed microchannels. Under enough packing length and appropriate packing position of micro-particles, the ideal micromixing performance could be obtained in packed microchannels. Furthermore, the micromixing time in packed microchannels was determined based on the incorporation model, and its value was in the range of 0–0.1 ms.

1. Introduction

Mixing in equipment includes macromixing, mesomixing, and micromixing, which are on different levels. Macromixing and mesomixing are coarse-scale processes, which both influence reactions indirectly by determining the environment where micromixing takes place. Micromixing is the mixing at the molecular scale, and is believed to play a very important role in the reaction process when the characteristics time scale of the chemical reaction involved is at the same magnitude or smaller than the time scale of the mixing process. Various reaction processes, such as polymerization (Engelmann and Schmidtnaake, 1994), self-catalysis (Bourne, 1983), enzyme catalytic reaction (Giridhar and Krishnaiah, 1993), and some parallel competing or consecutive reactions (Okubo and Mae, 2009) are strongly dependent on the micromixing efficiency. Specifically, the micromixing may control the molecular weight distribution in the polymerization, and it may greatly affect the selectivity and the yield for chemical reaction systems. Due to its importance on the process engineering, the development of novel reactors with enhanced micromixing efficiency is desirable. From stirred tanks (Assirelli et al., 2002; Yao et al., 1998) to turbulent tube reactors (Barresi et al., 1999), static mixers with inner construction (Liu et al., 2006), and micromixers, the reactor design for better mixing performance has developed quickly.

As one of the most important methods to intensify micromixing, microscale devices such as micromixers and microreactors have attracted increasing attention in both laboratories and commercial areas in recent years (Ehrfeld et al., 1999; Hessel and Löwe, 2003; Wiles and Watts, 2008, Wong et al., 2004). The values of Reynolds number are usually low in microstructure devices due to their small characteristic dimension; therefore, the flow in micromixers and microreactors is generally within the laminar flow regime, and the mixing is mainly driven by the molecular diffusion. Increase in the interfacial area of fluids, reduction of the diffusion length between fluids, and introducing advection are proved to be effective methods for improving the micromixing efficiency in micromixers (Hessel et al., 2005). By far, many micromixers with high micromixing efficiency have been proposed. Nagasawa et al. (2005) had designed a new type of micromixer for rapid mixing by both kinetic energy and molecular diffusion of fluids. The rapid mixing was realized by the collision of microfluidic segments, which were divided into several radial streams at the center of mixer. Ehrfeld et al. (1999) fabricated an interdigital micromixer with channel characteristic size of only 25 μm, and the fast mixing was obtained by using the principle of multilamination. Wong et al. (2004) demonstrated that the swaying of the fluids in the complicated twisted microchannel caused chaotic advection, hence improved the micromixing performance. The excellent micromixing performance could be achieved by flow splitting, recombination, and rearrangement in split-and-recombine micromixers (Schönfeld et al., 2004). However, it is difficult to manufacture these micromixers due to the complexity of their structure, and their practical application usually is scarce. T-shaped microchannel is easy to design and manufacture, so it is widely used in laboratory. Soleymani et al. (2008) carried out the numerical and experimental investigations of liquid mixing in T-shaped microchannels. Their simulation results proved that the occurrence and the development of vortices in the T-junction of the microchannel were essential for the good mixing performance, which both strongly depended on the flow

* Corresponding author. Tel.: +86 411 8437 9031; fax: +86 411 8469 1570.
E-mail address: gwchen@dicp.ac.cn (G. Chen).

0009-2509/$ - see front matter © 2011 Elsevier Ltd. All rights reserved.
doi:10.1016/j.ces.2011.03.024

rate, the aspect ratio, and the throttle size of the microchannel, and the angle of two inlet channels. Based on the results of the numerical simulations, they designed new micromixers with two junctions and circular elements in the mixing channel, and the experiments showed that the mixing performance of these new micromixers was significantly better than that of the ordinary T-shaped microchannels.

Besides designing complex structures, the mixing of the miscible liquid–liquid two phases in microchannels can be intensified effectively by introducing another immiscible phase to form multiphase flow. The mixing of multiple reagents was isolated in the liquid slugs by introducing the immiscible carrier phase in the winding microchannels, and the chaotic advection appeared in slugs by internal circulations, which could stretch and fold the fluids striation, eventually the intensification of the mixing in droplets could be obtained (Bringer et al., 2004). Reactions in slugs in microchannels have attracted many researchers due to the elimination of Taylor dispersion and the enhanced mixing performance by internal circulation, such as measurement of fast reaction kinetics parameters (Song and Ismagilov, 2003), protein crystallization (Zheng et al., 2004), synthesis of nanoparticles (Khan and Jensen, 2007), etc. Nevertheless, the multiphase flow approach involve the separation of the gas–liquid two phases or the liquid–liquid two phases after the outlet of the microchannel.

Seong and Crooks (2002) had reported a convenient and effective strategy for the mixing process in the microfluidic system by introducing solid microbeads. The catalysts were immobilized on the microbeads, and then the beads were placed into the well-defined zone of the microchannel. Their results demonstrated that the catalyst-modified beads increased the effective surface area of the microchannel interior for the mixing of reactants, and thus the reaction velocities were improved compared with the open microchannel. In earlier work, we had established a method to intensify the mixing and the mass transfer between the immiscible liquid–liquid two phases in microchannels by packing micro-particles (Su et al., 2010). In the packed microchannel, the parallel flow of the immiscible liquid–liquid two phases could easily transform to the dispersed droplets flow, which resulted in larger interfacial area and higher mass transfer rate.

The mixing mechanism and the research method for the homogeneous fluids are different from those for the heterogeneous fluids. In this work, the hydrodynamics and the micromixing performance in the packed and non-packed microchannels were studied experimentally at low Reynolds numbers in the range of 8–300. The mixing process between a colorless and a blue dye water solution was observed with the high-speed CCD camera. The micromixing efficiency in microchannels was evaluated with the widely used Villermaux/Dushman method. Moreover, the micromixing time was calculated based on the incorporation model. The effects of different operating conditions, such as the packing length and the packing position of microparticles, on the micromixing efficiency were investigated experimentally. For the convenience of comparison between the packed and non-packed microchannels, Reynolds number was used as the main parameter and defined based on the volume flux in the microchannel and the hydraulic diameter of the microchannel without considering the effect of packing micro-particles.

2. Experiments

2.1. Villermaux/Dushman reaction for quantitative research on micromixing

The micromixing performance of the mixers was evaluated by the Villermaux/Dushman method based on a parallel competing reaction system (Fournier et al., 1996a, b):

$$H_2BO_3^- + H^+ \rightarrow H_3BO_3 \text{ (quasi-instantaneous)} \quad (1)$$

$$5I^- + IO_3^- + 6H^+ \rightarrow 3I_2 + 3H_2O \text{ (very fast)} \quad (2)$$

$$I_2 + I^- \leftrightarrow I_3^- \quad (3)$$

The neutralization reaction (1) is quasi-instantaneous while the redox reaction (2) is fast but much slower than reaction (1). And reaction (3) is an instantaneous equilibrium reaction. Under perfect micromixing conditions, the injected acid is instantaneously dispersed in the reactive medium and consumed by borates according to reaction (1). Otherwise, the injected acid is consumed competitively by reactions (1) and (2), and the formed I_2 can further react with I^- to yield triiodide complex (I_3^-) according to reaction (3). The amount of I_3^- produced depends on the micromixing efficiency and can be easily measured by a spectrophotometer (4802UV/VIS) at 353 nm. The micromixing performance is less ideal, the more iodine is formed and the stronger light absorption (Abs) is detected. Based on the obtained concentration of I_3^-, the segregation index (X_s) that is defined to quantify the micromixing efficiency can be obtained:

$$X_s = \frac{Y}{Y_{ST}} \quad (4)$$

$$Y = \frac{2(V_1+V_2)([I_2]+[I_3^-])}{V_1[H^+]_0} \quad (5)$$

$$Y_{ST} = \frac{6[IO_3^-]_0}{6[IO_3^-]_0 + [H_2BO_3^-]_0} \quad (6)$$

Y is the ratio of acid mole number consumed by reaction (2) to the total acid mole number injected and Y_{ST} is the value of Y in the total segregation case when the micromixing process is infinitely slow. The value of X_s is within the range of $0 < X_s < 1$ for partial segregation, and X_s equates to 0 for ideal mixing, while X_s equates to 1 for total segregation, respectively.

In order to quantitatively research the micromixing performance in the packed and the non-packed microchannels, the relationship between the light absorption and the concentration of I_3^- was studied, and the mixed solutions of I_2/I^- with different concentrations were prepared to form the I_3^- solutions according to reaction (3). As shown in Fig. 1, there was a linear relationship between the absorbance and the concentration of I_3^-, which

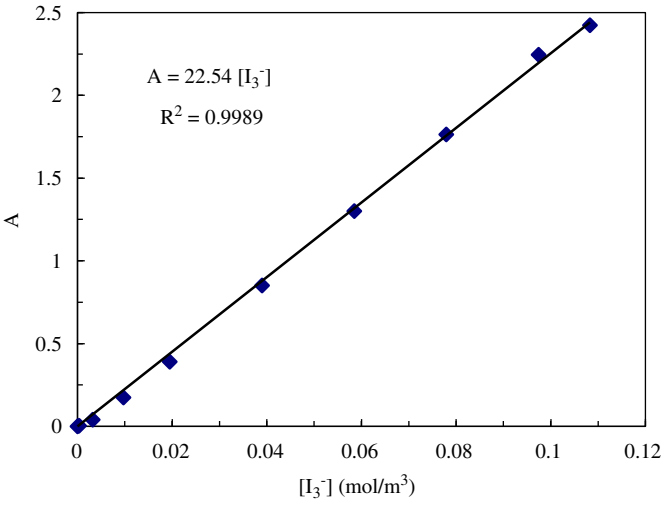

Fig. 1. Relationship of absorbance and concentration of the triiodide complex.

accorded with Lambert–Beer law and could be expressed as follows:

$$A = 22.54[I_3^-] \quad (7)$$

If the light absorption of solution was measured, the concentration of the triiodide complex could be back-calculated through Eq. (7). It deserves to be specially noted that the light absorption was not linearly related to the concentration of the triiodide complex any more when its value was more than 2.5. In addition, the light absorption was in the range of apparatus detection error when its value was less than 0.0010, at that time the concentration of the triiodide complex was considered as zero by the spectrophotometer.

2.2. Experimental procedure

The typical T-shaped microchannel was fabricated in the transparent PMMA substrate by micromachining technology (FANUC KPC-30a) in our CNC Machining Center. The depth, the width, and the length of the microchannel were 600 μm, 600 μm, and 70 mm, respectively. Another PMMA plate was used as a cover plate. The thickness of both PMMA plates was 9.6 mm. The quartz sand micro-particles were crystalline, their shape was irregular, and their average diameter was about 300 μm (Fig. 2(a)). These quartz sand micro-particles were packed elaborately by using a little spoon, and they contacted with each other and filled the microchannel without exceeding the edge of it. The packing length of micro-particles was approximately proportional

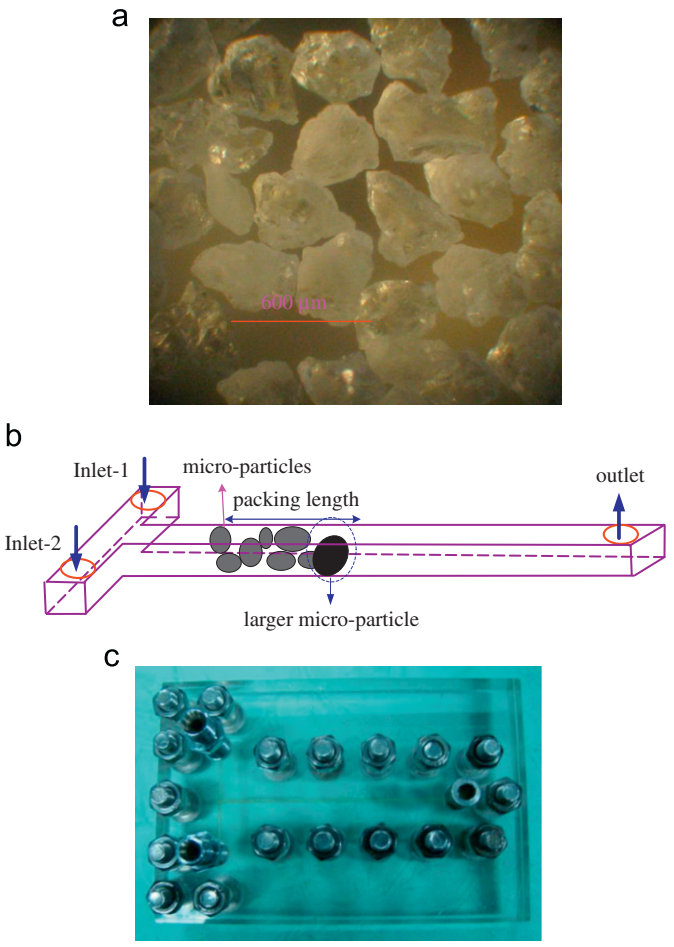

Fig. 2. (a) Picture of quartz sand micro-particles shot by a digital camera with microscope, (b) schematic diagram of packed microchannel, and (c) picture of packed microchannel mixer.

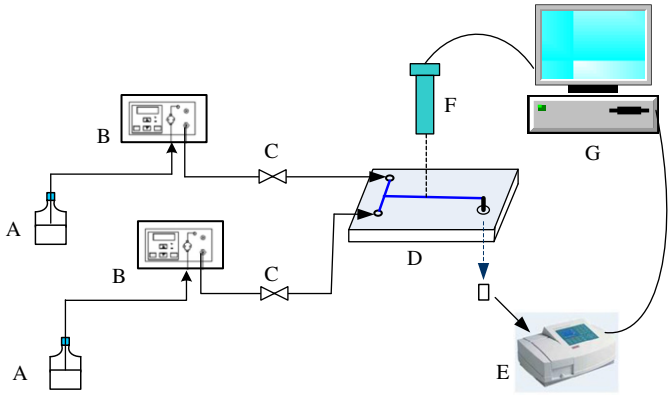

Fig. 3. Schematic diagram of experimental setup: (A) liquid tank, (B) piston pump, (C) check valve, (D) microchannel, (E) 4802UV/VIS spectrometer, (F) CCD camera, and (G) computer.

to the weight of micro-particles for the regularity and the reproduction, and the porosity was 0.64. To prevent the loss of micro-particles, a micro-particle whose diameter approximately equaled to the hydraulic radius of the microchannel was packed in the rear of the packing section as shown in Fig. 2(b). The width of the irregular big particle fitted the width of the channel so that both sides of the particle could contact closely with the microchannel wall and then the particle fixed itself in the channel. Because the big particle was irregular, so there was void for fluid flowing through. After packing micro-particles in the microchannel, the plates were compressed with each other by bolts. By this procedure, the micro-particles could not move freely in the microchannel, and finally the packed microchannel was built. The detailed procedure of the packed microchannel was also seen in our earlier study (Su et al., in press). The packed microchannel mixer is shown in Fig. 2(c).

The schematic diagram of experimental setup is shown in Fig. 3, solutions A and B were fed into the microchannels through two inlets by two high precision piston pumps (Beijing Satellite Manufacturing Factory, measurement range: 0.01–5 ml/min), and the volume flux ratio of solution A to solution B was fixed at 1. After collecting enough solution in a sample cell (about 3 ml), the concentration of I_3^- in the effluent was measured within 20 s by the spectrophotometer. In order to observe the mixing performance in microchannels, the solutions A and B were both replaced by de-ionized water, and minute amounts of methylene blue was dissolved in solution A for better visualization of the mixing phenomena. The characteristics of hydrodynamic and mixing could be observed with the high-speed CCD camera that was connected to a personal computer. All experiments were conducted at room temperature (27–28 °C). Solution A was a mixture of potassium iodate (0.00233 mol/l), potassium iodide (0.0115 mol/l), sodium hydroxide (0.125 mol/l), and boric acid (0.25 mol/l). Solution B was a dilute sulfuric acid solution, and its concentration was 0.0246 mol/l.

3. Results and discussion

3.1. Observations of the mixing process in microchannels

The transport processes such as mixing or heat transfer are greatly relevant to flow in devices. The flow in microchannels is generally regarded as laminar for straight channels with low Reynolds numbers. Fig. 4 shows the effects of Reynolds number on the mixing in the non-packed microchannel. From Fig. 4, it is seen that the two miscible phases flowed side-by-side in the non-packed microchannel, with presenting a distinct

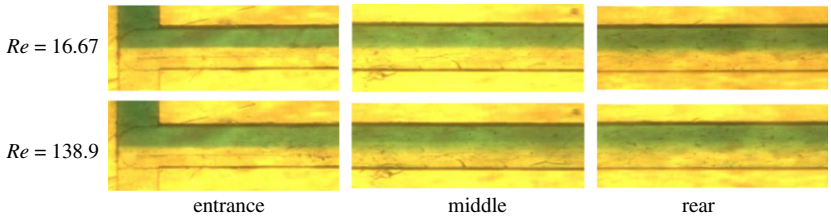

Fig. 4. Mixing performance in the non-packed microchannel.

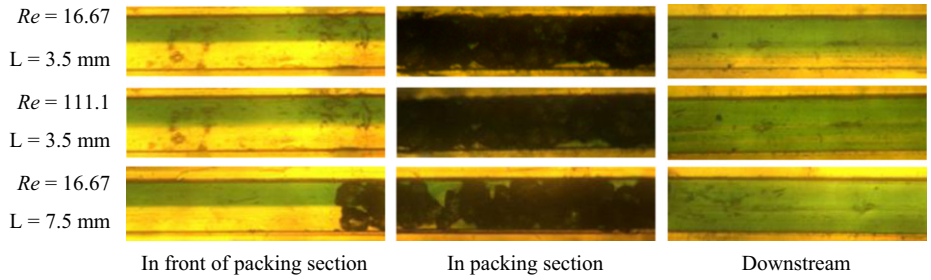

Fig. 5. Mixing performance in packed microchannels.

concentration interface between themselves even at the rear of the channel for two different Reynolds numbers (Re=16.67 and 138.9). The interface in the rear of the channel demonstrated that the mixing of the two miscible phases could not reach uniformity. For extremely low Reynolds number (Re=0.8), Gunther et al. (2005) had reported two streams containing 10-fold different concentrations of a fluorescent dye mixed by the diffusion in the microchannel, the required mixing length was substantially longer than 1.0 m.

Fig. 5 shows the mixing performance in packed microchannels for different Reynolds numbers and different packing lengths of micro-particles. In front of the packing section, there was a clear concentration interface between the miscible liquid–liquid two phases for two Reynolds numbers (Re=16.67 and 111.1). However, in the packing section the two miscible fluids flowed into the confined and crooked interstices between the micro-particles and mixed acutely. In the extremely narrow micro-space, the two miscible fluids interwove and sheared each other. The irregular micro-particles also sheared the fluids drastically, which was beneficial to the mixing of the two miscible fluids. The fluid elements underwent stretching and folding in the packed section, so the lateral flow and the maximum amount of interfacial area between the two initially segregated fluids were produced in the minimum amount of the time. It can be seen that the mixing performance was also dependent on the packing length of micro-particles. When the packing length equated to 7.5 mm, the mixing could reach homogeneous completely at the lower Reynolds number (Re=16.67).

3.2. Comparison of micromixing performance between packed and non-packed microchannels

The hydrodynamics in microchannels could be photographed by the high-speed CCD camera, thus the mixing process of the miscible liquid–liquid two phases could be visually observed. However, these high-speed imaging techniques could only provide information in macroscale or mesoscale. In the following sections, the micromixing performance in the packed and the non-packed microchannels was investigated by using the "Villermaux/Dushman" method.

Fig. 6 shows the comparison of the micromixing performance between the packed and the non-packed microchannels, in which

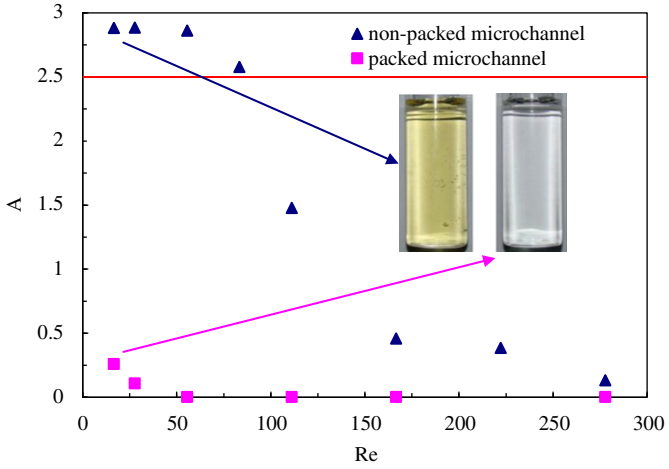

Fig. 6. Comparison of micromixing performance between the packed and non-packed microchannels. (For interpretation of the references to color in this figure legend, the reader is referred to the web version of this article.)

the light absorption was used. The weight of micro-particles was 2.5 mg, the packing length was 7.5 mm, and the distance between T-junction and the threshold of the packing section was 4.5 mm. It is seen the light absorption in the packed microchannel was much lower than that in the non-packed microchannel, and its value was even as low as 0.0014. The extremely low light absorption in the packed microchannel demonstrated that a much better micromixing efficiency could be obtained compared with the non-packed microchannel. This situation was more obvious as the value of Re was well below 100. For the non-packed microchannel, the light absorptions of the points above the red line were all more than 2.5, and not linearly related to the concentration of I_3^- any more. Actually, the phenomena with low micromixing efficiency could be visually judged from the yellow effluent due to the formation of more iodine in the mixing process. For example, with the same value of low Reynolds number (Re=16.67), the outlet solution from the non-packed microchannel was yellow, however, it was transparent from the packed microchannel, as also shown in Fig. 6.

The excellent micromixing performance in the packed microchannel was relevant to the hydrodynamic characteristics.

As discussed above, in the packing section the miscible liquid–liquid two phases flowed into the confined and crooked interstices between micro-particles and mixed acutely. In the extremely narrow micro-space, the two miscible fluids interwove and sheared each other, and the irregular micro-particles also sheared the fluids drastically; therefore, the fluid elements were stretched, folded and sheared, and thinner striation thickness and larger interfacial area for mass transfer were generated. Furthermore, it was forecasted that the chaotic advection could occur easily in the packing section of the packed microchannel. A necessary condition for the chaotic advection in the microfluidics was that the two successive streamline portraits should show intersecting streamlines at the moving direction when projected onto the cross sectional plane (Ottino and Wiggins, 2004). The packed micro-particles made the fluids to distribute in the cross-section of the microchannel with a random manner, that is, the lateral flow and the chaotic advection appeared spontaneously. Finally, the concentration gradient, the mass flux, and the micromixing efficiency were increased.

At the microscale, the mixing can only be accomplished through the molecular diffusion, and one of the most favorable methods to improve the mixing performance is the static mixer approach. Static mixers do not require any moving part, and the mixing is not obtained by any external agitation, but by the natural motion of the fluid as it flows through the mixing elements composing the static mixer. Actually, the packed microchannel can be considered as a static micromixer, where the perfect micromixing can be obtained.

The much excellent micromixing performance in the packed microchannel was at the expense of the increased pressure drop, which was relevant to the specific energy dissipation. In previous work (Su et al., 2010), we had investigated the pressure drop characteristics in the packed microchannel, and the pressure drop was much higher than that in the non-packed microchannel because of the friction force between fluids and the micro-particles, the impinging of fluids on micro-particles and the sudden expansion or reduction of cross-section. Furthermore, the specific energy dissipation in the packed microchannel was considered at the same order of magnitude compared with static mixers. An empirical correlation had also been proposed for estimating the pressure drop of the immiscible liquid–liquid two phases in the packed microchannel. Here, we use the correlation to approximately predict the pressure drop in the packed microchannel for this miscible liquid–liquid two-phase system. For the packing length of 7.5 mm the pressure drop was speculated in the range of from 2.2 to 50.2 kPa according to the superficial velocity from 0.0278 to 0.463 m/s (*Re*: 16.67–277.78).

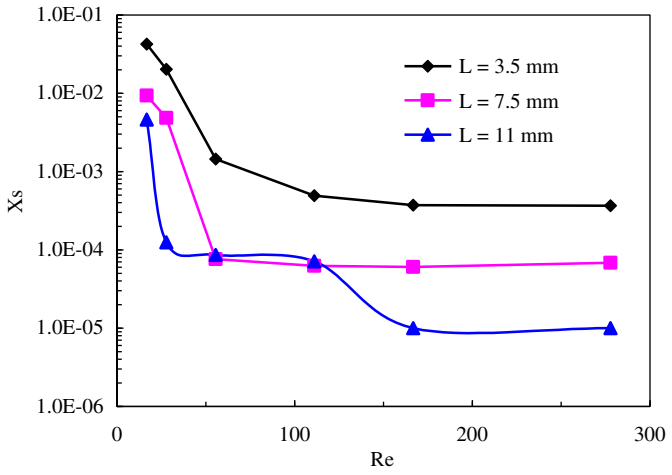

Fig. 7. Effect of packing length on X_s.

3.3. Effect of packing length on micromixing performance

The packing length of micro-particles has an influence on the hydrodynamics and the mixing performance. The effects of the packing length of micro-particles on X_s in the packed microchannel are shown in Fig. 7. The distance between the T-junction of the microchannel and the threshold of the packing section for different packing length was 4.5 mm. It can be seen that X_s decreased with increasing in packing length, and tended to be smaller until Reynolds number reached a certain value. The effect of the packing length on X_s was relatively small when the Reynolds number was larger than 100. The value of X_s was as low as 0 for the longest packing length (L=11 mm), which indicated that the ideal micromixng could be easily obtained in the packed microchannel. The thickness of the fluid striation laminae was dependent on the Reynolds number and the packing length in packed microchannels, that is, the micromixing efficiency was the coupling of Reynolds number and the packing length. The fluid elements were further sheared, stretched, and folded with an increase in the packing length of micro-particles, and thus larger effective interfacial area could be obtained. It is well known that the distance between striations is inversely proportional to the surface area: the thinner the striations, the faster the diffusion. Therefore, the concentration gradient and the mass flux increased with increasing in packing length of micro-particles, and finally the micromixing performance was further intensified. As the Reynolds number reached a certain value, even a few micro-particles could make fluid elements to be divided up sufficiently and mix drastically. Under this situation, the effect of the packing length on the micromixing performance was relatively weak. In addition, an increase in the packing length of micro-particles must lead to higher pressure drop in packed microchannels (Su et al., 2010), so the packing length of micro-particles and the micromixing performance should match each of the optimal designs of the packed microchannel.

3.4. Effect of packing position on micromixing performance

The zone of the T-junction in the T-shaped microchannel was of the greatest importance, and the vortices maybe occur and develop in this zone, which were essential for the good mixing performance (Soleymani et al., 2008). In order to investigate the effect of the micro-particles packing position on X_s, three different packing positions of micro-particles were chosen, as shown in Fig. 8. The packing length was kept constant (L=7.5 mm), and the

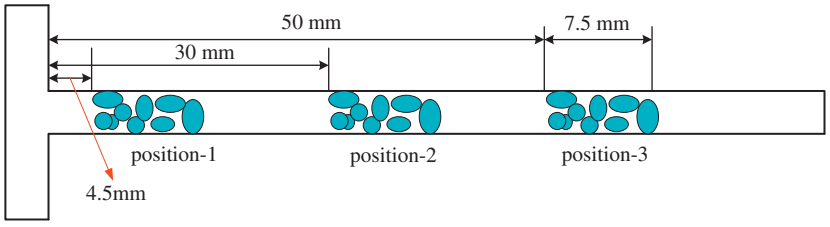

Fig. 8. Schematic diagram of three different packing positions.

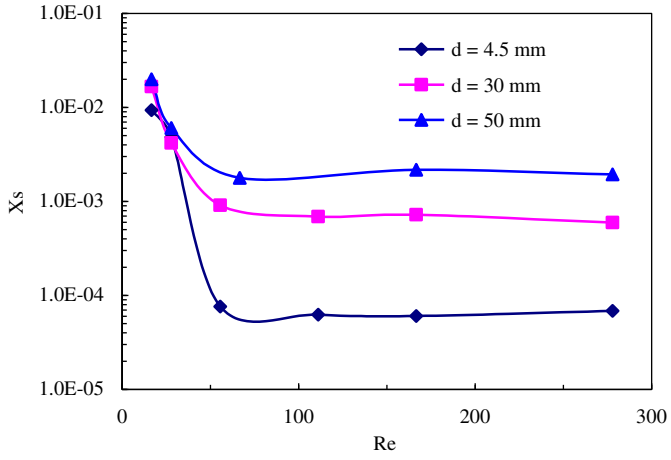

Fig. 9. Effect of packing position on X_s.

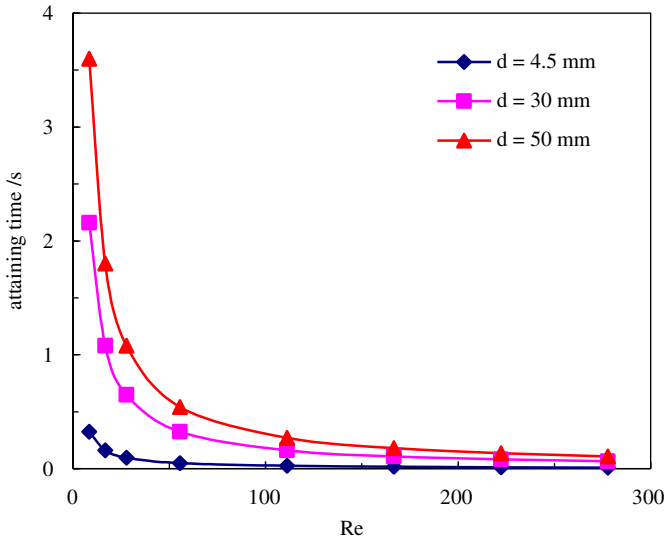

Fig. 10. Effect of packing position on t_a.

distances between T-junction and the threshold of the packing section (d) for the same packing length were 4.5, 30, and 50 mm, respectively. From Fig. 9, it can be seen that X_s was dependent on the packing position, and the micromixing efficiency was higher for position-1. That is, the best location for the packed bed in the packed microchannel is just after the impact of the fluids. From the above discussion, the miscible liquid–liquid two phases flowed side-by-side, and the mixing between them was through the molecular diffusion, thus it was hard to reach homogeneous before the fluids entered the packing section. The micromixing efficiency in this section was much inferior to that in the packing section. When the micro-particles were packed in position-1, the miscible two fluids could quickly reach the packing section, and the perfect micromixing condition could be obtained, resulting in lower values of X_s. In addition, if the distance between T-junction and the threshold of the packing section was longer, there was more specific energy dissipation before the fluids entered the packing zone. In other words, the energy of fluids entering the packing section was lower, which was not beneficial to the mixing in the packing section. Actually, the specific energy dissipation in microchannels is complicated and relevant to the drop pressure and the micromixing performance. Therefore, a detailed investigation of the specific energy dissipation in packed microchannels and its interaction with the mixing phenomenon is necessary to optimize the design of the packed microchannel, and will be discussed in the future work.

The effect of the packing position on X_s became less pronounced as Reynolds number became larger. The reason is that the difference of the attaining time (t_a) was reduced with the increase in Reynolds number. Here, the attaining time referred to the time during the fluids flowing through the distance between the T-junction and the threshold of the packing section. Fig. 10 shows the effect of Reynolds number on the attaining time. It is clear that the difference in the attaining times for different positions was greatly reduced as Reynolds number was larger than 100. That is, the fluids could quickly reach the packing section for all three packing positions. The difference in the mircomixing efficiency between the packed and the non-packed microchannels was also decreased as the Reynolds number reached a certain value. Therefore, the effect of the micro-particles packing position was weaker as Reynolds number became larger.

3.5. Calculation of micromixing time in packed microchannels

It is well known that the characteristic reaction time and the characteristic micromixing time (t_m) compete between themselves when fast reactions occur in reactors. The characteristic reaction time and the characteristic micromixing time are dependent on the intrinsic kinetics and the hydrodynamic condition, respectively. The characteristic micromixing time is usually requested to be smaller than the characteristic reaction time for higher yield and selectivity in the fast reaction systems, such as enzymic catalytic reaction, consecutive reaction, etc. Many models had been proposed to calculate the micromixing time from the segregation index, such as the IEM model developed by Villermaux and Devillon (1972), and droplet erosion and diffusion model reported by Ou and Ranz (1983), the engulfment deformation diffusion model reported by Baldyga and Bourne (1990), and the incorporation model (Fournier et al., 1996a, b). Among these models, the incorporation model is believed to be simple and widely used for estimating the micromixing time in many kinds of reactors including microchannel reactors (Wu et al., 2009; Yang et al., 2009). In the incorporation model an incoming fluid (sulfuric acid solution, B) is divided into series of aggregates, which interact with the surrounding fluid (solution A). The isolated aggregates grow progressively by incorporating the surrounding fluid, in the meantime reactions (1) and (2) occur. The characteristic time of incorporation is considered to be equal to the micromixing time. The equations of the incorporation model are given by:

$$\frac{dC_j}{dt} = \frac{1}{g(t)}\frac{dg(t)}{dt}(C_{j0} - C_j) + R_j \tag{8}$$

where C_j denotes the concentration of reactants ($H_2BO_3^-$, H^+, I^-, IO_3^-, I_2, I_3^-), C_{j0} represents the initial concentration of j ion in solution A. R_j is the net production rate of species j for the reaction. The available growth law of aggregates is a function of t_m:

$$g(t) = \exp(t/t_m) \tag{9}$$

Then

$$\frac{dC_j}{dt} = \frac{C_{j0} - C_j}{t_m} + R_j \tag{10}$$

The equations can be solved by the Runge–Kutta method, and the detailed process was reported by Yang et al. (2005). The integration ends as the concentration of H^+ approaches zero. By assuming a series of t_m, the concentrations of species can be calculated, and then X_s can be calculated according to its definition.

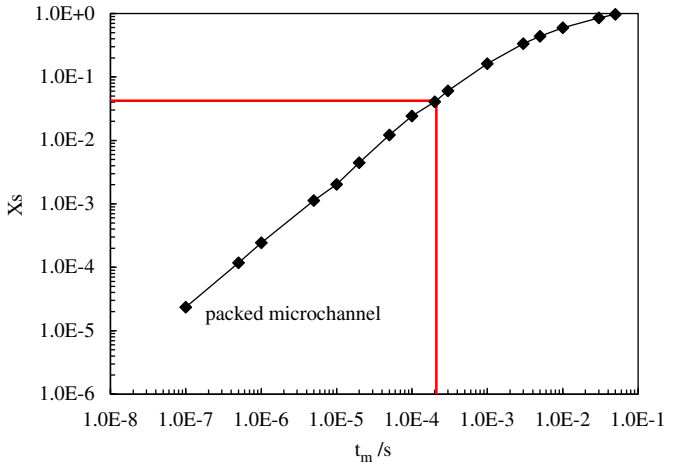

Fig. 11. Relationship between t_m and X_s (C_{H^+} =0.0492 mol/l).

Fig. 11 shows the theoretical relationship between X_s and t_m based on the incorporation model at the same condition with experimental results of Fig. 7. According to the experimental values of X_s, it was observed that t_m was in the range of 0–10^{-4} s for packed microchannels. As t_m equaled to zero, at that time the ideal micromixing could be obtained. The extremely low t_m also provides a new approach for studying the ultra-fast reaction kinetics. For the kinetic measurements of ultra-fast reactions, the mixing needs to be completed instantaneously before the reactions occur.

4. Conclusions

The hydrodynamics and the micromixing characteristics in the packed and non-packed microchannels were investigated by high-speed imaging techniques and Villermaux/Dushman method, respectively. From the observation of the hydrodynamics, it is seen that the mixing of miscible liquid–liquid two phases was dependent on the packing length of micro-particles in the packed microchannel. As the same as the macromixing (or mesomixing), the micromixing performance in the packed microchannel was improved obviously compared with the non-packed microchannel. The reason is that the fluid elements were stretched, folded, and sheared with the effects of micro-particles in packed microchanels, resulting in much shorter diffusion distance and larger effective interfacial area. In particular, increasing the packing length and decreasing the distance between T-junction and the threshold of the packing section were both beneficial to the micromixing performance in packed microchannels, and the ideal micromixing could be obtained under enough packing length and appropriate packing position of micro-particles. The micromixing time in microchannels was also evaluated based on the incorporation model, and its value was in the range of 0–10^{-4} s. The extremely low t_m also provides a new approach for studying the ultra-fast reaction kinetics.

Nomenclature

A	reactive solution which contains $H_2BO_3^-$, I^-, and IO_3^-
B	H_2SO_4 solution
C_j or $[j]$	concentration of species j (mol/l)
C_{j0}	environmental concentration of species j (mol/l)
d	distance between T-junction and threshold of packing section (mm)
$g(t)$	growth function of incorporation law
L	packing length of micro-particles (mm)
Re	Reynolds number, 1
R_j	rate of the reaction j (mol/l)/s
t	time (s)
t_m	micromixing time (s)
t_a	time during fluids flowing though the distance between T-junction and threshold of packing section (s)
V_A	volumetric flow rate of A (ml/min)
V_B	volumetric flow rate of B (ml/min)
X_s	segregation index, 1
Y	ratio of acid mole number consumed by reaction (2) to the total acid mole number injected, 1
Y_{ST}	value of Y in the total segregation case, 1

Acknowledgments

The work reported in this article was financially supported by research grants from the National Natural Science Foundation of China (no. 20906087), and the framework of the Sino-French project MIGALI via the National Natural Science Foundation of China (no. 20911130358), Fund of Dalian Institute of Chemical Physics, CAS (no. K2009D01).

References

Assirelli, M., Bujalski, W., Eaglesham, A., Nienow, A.W., 2002. Study of micromixing in a stirred tank using a Rushton turbine—comparison of feed positions and other mixing devices. Chemical Engineering Research and Design 80, 855–863.
Baldyga, J., Bourne, J.R., 1990. Comparison of the engulfment and the interaction-by-exchange-with-the-mean micromixing models. Chemical Engineering Journal and the Biochemical Engineering Journal 45, 25–31.
Barresi, A.A., Marchisio, D., Baldi, G., 1999. On the role of micro- and mesomixing in a continuous Couette-type precipitator. Chemical Engineering Science 54, 2339–2349.
Bourne, J.R., 1983. Mixing on the molecular scale (micromixing). Chemical Engineering Science 38, 5–8.
Bringer, M.R., Gerdts, C.J., Song, H., Tice, J.D., Ismagilov, R.F., 2004. Microfluidic systems for chemical kinetics that rely on chaotic mixing in droplets. Philosophical Transactions of the Royal Society of London Series A—Mathematical Physical and Engineering Sciences 362, 1087–1104.
Ehrfeld, W., Golbig, K., Hessel, V., Löwe, H., Richter, T., 1999. Characterization of mixing in micromixers by a test reaction: single mixing units and mixer arrays. Industrial and Engineering Chemistry Research 38, 1075–1082.
Engelmann, U., Schmidtnaake, G., 1994. Influence of micromixing on the free-radical polymerization in a discontinuous process. Macromolecular Theory and Simulations 3, 855–883.
Fournier, M.C., Falk, L., Villermaux, J., 1996a. A new parallel competing reaction system for assessing micromixing efficiency—experimental approach. Chemical Engineering Science 51, 5053–5064.
Fournier, M.C., Falk, L., Villermaux, J., 1996b. A new parallel competing reaction system for assessing micromixing efficiency—determination of micromixing time by a simple mixing model. Chemical Engineering Science 51, 5187–5192.
Giridhar, M., Krishnaiah, K., 1993. The effect of micromixing and macromixing on enzyme reaction in a real Cstr. Bioprocess Engineering 9, 263–269.
Gunther, A., Jhunjhunwala, M., Thalmann, M., Schmidt, M.A., Jensen, K.F., 2005. Micromixing of miscible liquids in segmented gas–liquid flow. Langmuir 21, 1547–1555.
Hessel, V., Löwe, H., 2003. Microchemical engineering: components, plant concepts user acceptance—part I. Chemical Engineering and Technology 26, 13–24.
Hessel, V., Löwe, H., Schönfeld, F., 2005. Micromixers—a review on passive and active mixing principles. Chemical Engineering Science 60, 2479–2501.
Khan, S.A., Jensen, K.F., 2007. Microfluidic synthesis of titania shells on colloidal silica. Advanced Materials 19, 2556–2560.
Liu, S.P., Hrymak, A.N., Wood, P.E., 2006. Laminar mixing of shear thinning fluids in a SMX static mixer. Chemical Engineering Science 61, 1753–1759.
Nagasawa, H., Aoki, N., Mae, K., 2005. Design of a new micromixer for instant mixing based on the collision of micro segments. Chemical Engineering and Technology 28, 324–330.
Okubo, Y., Mae, K., 2009. Process intensification using a two-phase system and micromixing for consecutive and reversible reactions. AIChE Journal 55, 1505–1513.
Ottino, J.M., Wiggins, S., 2004. Introduction: mixing in microfluidics. Philosophical Transactions of the Royal Society of London Series A—Mathematical Physical and Engineering Sciences 362, 923–935.
Ou, J.J., Ranz, W.E., 1983. Mixing and chemical-reactions—a contrast between fast and slow reactions. Chemical Engineering Science 38, 1005–1013.

Schönfeld, F., Hessel, V., Hofmann, C., 2004. An optimised split-and-recombine micro-mixer with uniform 'chaotic' mixing. Lab on a Chip 4, 65–69.

Seong, G.H., Crooks, R.M., 2002. Efficient mixing and reactions within microfluidic channels using microbead-supported catalysts. Journal of the American Chemical Society 124, 13360–13361.

Soleymani, A., Kolehmainen, E., Turunen, I., 2008. Numerical and experimental investigations of liquid mixing in T-type micromixers. Chemical Engineering Journal 135, S219–S228.

Song, H., Ismagilov, R.F., 2003. Millisecond kinetics on a microfluidic chip using nanoliters of reagents. Journal of the American Chemical Society 125, 14613–14619.

Su, Y.H., Zhao, Y.C., Chen, G.W., Yuan, Q., 2010. Liquid–liquid two-phase flow and mass transfer characteristics in packed microchannels. Chemical Engineering Science 65, 3947–3956.

Su, Y.H., Zhao, Y.C., Jiao, F.J., Chen, G.W., Yuan, Q. The intensification of rapid reactions for multiphase systems in a microchannel reactor by packing microparticles. AIChE Journal, in press, doi:10.1002/aic.12367.

Villermaux, J., Devillon, J.C., 1972. Représentation de la coalescence et de la redispersion des domaines de ségrégation dans un fluide par un modéled'interaction phénoménologique. In: Proceedings of the 2nd International Symposium on Chemical Reaction Engineering; Amsterdam.

Wiles, C., Watts, P., 2008. Continuous flow reactors, a tool for the modern synthetic chemist. European Journal of Organic Chemistry, 1655–1671.

Wong, S.H., Ward, M.C.L., Wharton, C.W., 2004. Micro T-mixer as a rapid mixing micromixer. Sensors and Actuators B—Chemical 100, 359–379.

Wu, Y., Hua, C., Li, W.L., Li, Q., Gao, H.S., Liu, H.Z., 2009. Intensification of micromixing efficiency in a ceramic membrane reactor with turbulence promoter. Journal of Membrane Science 328, 219–227.

Yang, H.J., Chu, G.W., Zhang, J.W., Shen, Z.G., Chen, J.F., 2005. Micromixing efficiency in a rotating packed bed: experiments and simulation. Industrial and Engineering Chemistry Research 44, 7730–7737.

Yang, K., Chu, G.W., Shao, L., Xiang, Y., Zhang, L.L., Chen, J.F., 2009. Micromixing efficiency of viscous media in micro-channel reactor. Chinese Journal of Chemical Engineering 17, 546–551.

Yao, W.G., Sato, H., Takahashi, K., Koyama, K., 1998. Mixing performance experiments in impeller stirred tanks subjected to unsteady rotational speeds. Chemical Engineering Science 53, 3031–3040.

Zheng, B., Tice, J.D., Roach, L.S., Ismagilov, R.F., 2004. A droplet-based, composite PDMS/glass capillary microfluidic system for evaluating protein crystallization conditions by microbatch and vapor-diffusion methods with on-chip X-ray diffraction. Angewandte Chemie—International Edition 43, 2508–2511.